RESEARCH ARTICLE

Improved chromium reduction and removal from wastewater in continuous flow bioelectrochemical systems

Shashikanth Gajaraj [1,2] · Xining Sun [3] · Chiqian Zhang [1,4] (ID) · Zhiqiang Hu [1]

Abstract

Bioelectrochemical systems (BESs) including microbial electrolysis cells (MECs) and microbial fuel cells (MFCs) are promising for hexavalent chromium [Cr(VI)] reduction and total chromium (Cr) removal from wastewater. This study assessed the performance of simple, inexpensive, and continuous flow BESs with neither cathode catalyst nor proton exchange membrane for Cr(VI) reduction and total Cr removal. The effect of bioreactor configuration and wastewater feed mode on the performance of the BESs was investigated. Biological Cr(VI) reduction in the MEC followed a first-order kinetics with a rate constant of 0.103 d^{-1}, significantly higher than that of the control (0.033 d^{-1}). For comparison, the first-order reduction rate constants in the MFCs with Cr(VI) fed to the anodic and the cathodic zones were 0.072 and 0.064 d^{-1}, respectively. The BESs improved total Cr removal through coprecipitating Cr(III) and phosphors as evidenced from the scanning electron microscopy energy-dispersive X-ray spectroscopy analysis. The total Cr removal efficiencies in the control, MFCs, and MEC were 26.1%, 56.7%, and 66.2%, respectively. Only 25.1% to 26.7% of total Cr was present intracellularly in the BESs (both MFCs and MEC), whereas 31.8% ± 1.4% and 38.0% ± 0.9% of total Cr in the anodic and cathodic zones of the control were present intracellularly. Overall, the BESs demonstrated a great potential to reduce Cr(VI) and remove total Cr with the MEC having the fastest Cr(VI) reduction and most efficient total Cr removal. Furthermore, the BESs significantly reduced the intracellular total Cr content.

Keywords Microbial fuel cell · Microbial electrolysis cell · Bioelectrochemical systems · Hexavalent chromium · Coprecipitation · Wastewater

Introduction

Chromium (Cr) is widely used in industries including electroplating, alloys manufacturing, tanning, and wood pro-

✉ Chiqian Zhang
czxr9@mail.missouri.edu

✉ Zhiqiang Hu
huzh@missouri.edu

[1] Present address: Department of Civil & Environmental Engineering, University of Missouri, Columbia, MO 65211, USA

[2] Present address: HDR, Inc., Kansas City, MO 64131, USA

[3] College of Natural Resources and Environment, Northwest A&F University, Yangling 712100, Shaanxi, People's Republic of China

[4] Present address: School of Civil and Environmental Engineering, Georgia Institute of Technology, Atlanta, GA 30332, USA

cessing. Trivalent chromium [Cr(III)] is generally insoluble in ambient water and less toxic, whereas hexavalent chromium [Cr(VI)] is highly soluble and carcinogenic (Eary and Rai 1987, Hosseini and Belador 2009, Ishibashi et al. 1990, Mandiwana et al. 2007, Rai et al. 1989). Existing Cr removal techniques heavily rely on physicochemical processes such as adsorption and/or coprecipitation (Liu et al. 2014, Mohan and Pittman Jr 2006, Qin et al. 2005, Wu et al. 2018), reduction (e.g., by zero-valent iron) (Buerge and Hug 1997, Xu et al. 2018, Zhou et al. 2018), electrocoagulation (Al-Shannag et al. 2015, Cheballah et al. 2015, Lu et al. 2016), and electrolysis (Rutigliano et al. 2008). On the other hand, biological Cr(VI) reduction with the formation of Cr(III) precipitates is a promising alternative to remove Cr from wastewater (Chen and Hao 1998, Gupta et al. 2017, Habibul et al. 2016, Huang et al. 2015, Song et al. 2016, Wang et al. 2017). Microorganisms such as *Shewanella oneidensis* can reduce Cr(VI) and other mobile heavy metal species (Han et al. 2016, Lovley et al. 1991, Tebo and Obraztsova 1998). In situ

Cr remediation with a wide range of bacteria is therefore feasible (Liu et al. 2002, Schmieman et al. 1998), during which bacterial consortia including sulfate-reducing bacteria (SRB) and denitrifiers reduce Cr(VI) at Cr concentrations up to 70 mg L^{-1} under anaerobic conditions (Arias and Tebo 2003, Vainshtein et al. 2003). In bioreactors, Cr(VI) can be reduced at 80 mg L^{-1} without significantly inhibiting reactor performance (Vaiopoulou and Gikas 2012). Microbial reduction of Cr(VI) followed by Cr(III) coprecipitation is therefore promising, which could be further improved in bioelectrochemical systems (BESs) through enhanced electron-transferring (Li et al. 2018, Nancharaiah et al. 2015, Tandukar et al. 2009).

BESs including microbial fuel cells (MFCs) and microbial electrolysis cells (MECs) facilitate the reduction of electron acceptors such as Cr(VI) on the cathode and the oxidization of organic matter on the anode (Gupta et al. 2017, Habibul et al. 2016, Huang et al. 2015, Song et al. 2016). Therefore, BESs not only convert organic matter into energy (e.g., electricity) but also reduce, remove, and/or recover heavy metals, radionuclides, and recalcitrant chemicals (Gregory and Lovley 2005, Huang et al. 2011b, Nancharaiah et al. 2015, Wang et al. 2015, Wang and Ren 2014). Equation 1 shows the reduction of Cr(VI) on the cathode in BESs (Pandit et al. 2011):

$$Cr_2O_7^{2-} + 14H^+ + 6e^- \rightarrow Cr_2O_3 + 4H_2O$$
$$+ 6H^+ \rightarrow 2Cr^{3+} + 7H_2O \tag{1}$$
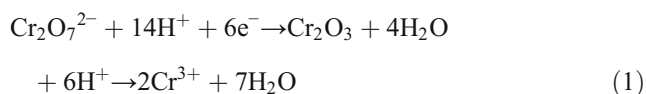
MFCs promote microbial Cr(VI) reduction (Li et al. 2008, Wang et al. 2008). For instance, the cathode of an MFC facilitated Cr(VI) reduction at pH 7, suggesting the involvement of Cr reducing bacteria (Tandukar et al. 2009) and/or electrochemically active exoelectrogens (Huang et al. 2010, Liu et al. 2011). Coupled with an adaptive procedure, an MFC reduced Cr(VI) at 1.24 mg L^{-1} h^{-1} (Huang et al. 2015). In another MFC with aluminum/nickel nanoparticle–dispersed carbon nanofiber electrode, Cr(VI) at an initial concentration of 100 mg L^{-1} was completely removed at a high Cr(VI) reduction rate of 2.13 mg L^{-1} h^{-1} (Gupta et al. 2017). MECs also facilitate Cr(VI) reduction. For example, an MEC at an external potential of −300 mV promoted the formation of biocathode and resulted in promising Cr(VI) reduction (Huang et al. 2011a).

The BESs for Cr(VI) reduction in previous studies are often operated in a batch mode; however, wastewater treatment facilities for field use is operated under a continuous mode. Previous research also used small BES volumes to determine Cr(VI) reduction and total Cr removal efficiency, whereas the performance of large, inexpensive BESs is still poorly evaluated. More importantly, the fate of Cr and its removal mechanisms in the BESs are not well understood. This study, therefore, aimed to assess the efficiency of simple, large bench-

scale, and continuous flow BESs in reducing Cr(VI) and removing total Cr. To better understand the Cr removal mechanisms, this study also determined Cr partitioning within bacterial cells (i.e., intracellular vs. extracellular total Cr), distribution in the biomass, and deposition on electrodes.

Materials and methods

Design and operation of BESs

Four identical bioreactors were constructed using window pane glass (Fig. 1). Each bioreactor had an effective working volume of 3.4 L, and was divided into three zones using plastic baffles suspended 1 cm above the bottom: an anodic zone (far left), a cathodic zone (middle), and an internal settling zone (far right). The anodic, cathodic, and settling zones had effective working volumes of 1.4, 1.4, and 0.6 L, respectively. The BESs were covered with Plexiglas plates and run in one of the following configurations:

- Control operated under open-circuit conditions
- MFC with Cr(VI) fed to the anodic zone
- MFC with Cr(VI) fed to the cathodic zone
- MEC with Cr(VI) fed to the anodic zone

Two anodes and two cathodes were used in each configuration by wrapping carbon fiber/graphite cloth (Plantraco Ltd., Saskatoon, Canada) (plain weave checkerboard pattern with a surface density of 0.08 kg m^{-2} and a resistivity of 10^{-5} Ω m) (Gajaraj and Hu 2014) over reticulated vitreous carbon (ERG, Oakland, CA) (8 pores per centimeter with a specific surface area of 114 m^2 m^{-3}). Each electrode had dimensions of 5 × 5 × 1.3 cm, a net volume of 130 cm^3, and a surface area of 148 cm^2. The anode and cathode were positioned approximately 5 cm apart, across the separating baffle plate. The electrodes in the MFCs were connected across a 1000 Ω resistor. In the MEC, a 10 Ω resistor was connected in series with the power supply, and a fixed voltage of 300 mV was applied to the circuit by connecting a potentiostat (model 3645A, Circuit Specialists, Inc., AZ). The voltage of the MEC was measured across the resistor.

The BESs were seeded with activated sludge from the Columbia Regional Wastewater Treatment Plant (Columbia, MO), operated at 23 ± 1 °C, and continuously fed with synthetic wastewater at a flow rate of 1.9 L d^{-1}, resulting in a 1.5-d hydraulic retention time (HRT). The synthetic wastewater was prepared following previous studies (Gajaraj and Hu 2014, Liang and Hu 2012). The concentrations of COD (glucose as the main source), NH_4^+-N, and total phosphorus (TP) of the synthetic wastewater were 500, 20, and 6 mg L^{-1}, respectively. The synthetic wastewater also contained 44 mg
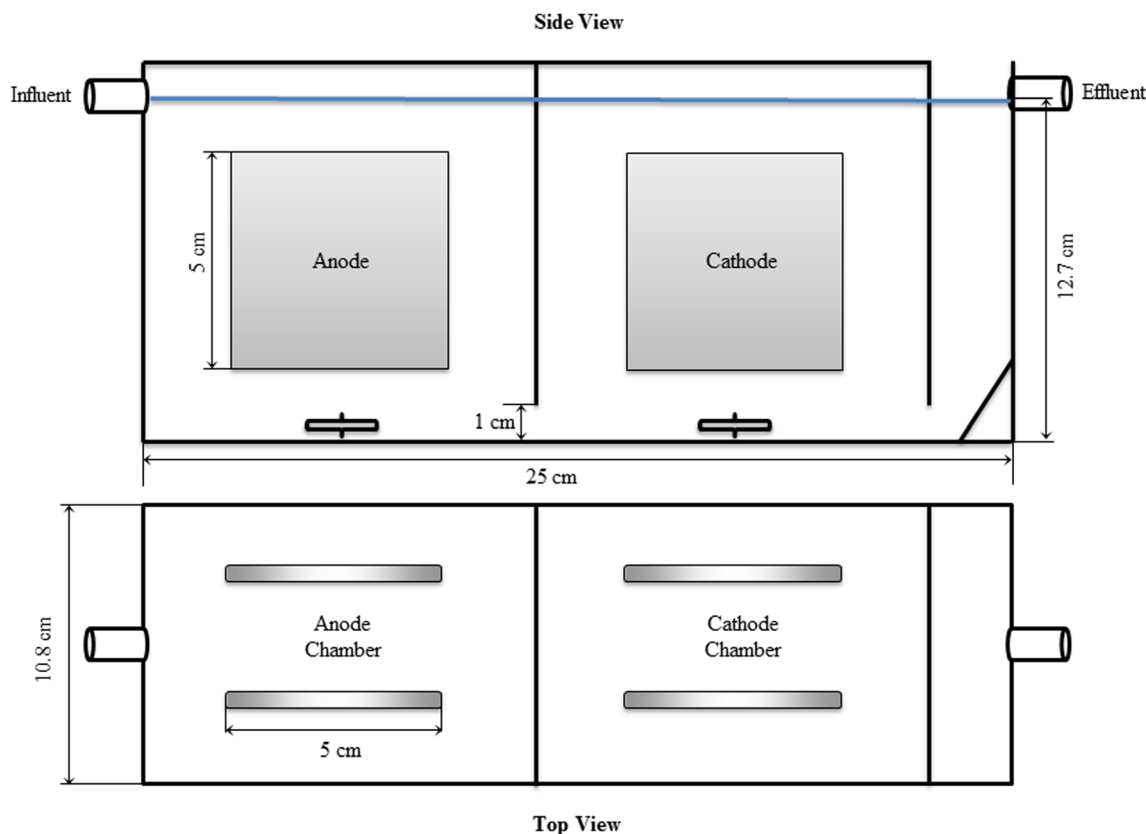
Side View

Fig. 1 A schematic of the continuous flow BESs for Cr(VI) reduction and total Cr removal.

L^{-1} of MgSO$_4$, 15 mg L^{-1} of CaCl$_2$·2H$_2$O, 2 mg L^{-1} of FeCl$_2$· 4H$_2$O, 3.4 mg L^{-1} of MnSO$_4$·H$_2$O, 1.2 mg L^{-1} of (NH$_4$)$_6$Mo$_7$O$_{24}$·4H$_2$O, 0.8 mg L^{-1} of CuSO$_4$, and 1.8 mg L^{-1} of Zn(NO$_3$)$_2$·H$_2$O. The influent was fed into the anodic zone, and the effluent left the bioreactor from the settling zone (Fig. 1). Magnetic stirrers ensured complete mixing of the mixed liquor in the anodic and cathodic zones. The mixed liquor returned to the cathodic zone from the settling zone via internal recirculation. Sludge was wasted from the settling zone to maintain a biomass concentration of approximately 2500 mg COD L^{-1} and an average solids retention time (SRT) of 10 d.

The BESs were operated for 25 d (day 0 to 25) before dosing the Cr(VI) feed stock at a fixed flow rate of 20 mL d^{-1}. The Cr(VI) feed stock concentration gradually increased from 100 to 1000 mg L^{-1}, resulting in influent nominal Cr(VI) concentration increased from 1 to 10 mg L^{-1}. The MEC was operated as an MFC for the first 15 d (day 0 to 15) before applying the external potential (300 mV).

Voltage generated by the MFCs was monitored across the 1000 Ω resistor at 1 Hz with a LabView software (National Instruments, TX), and the voltage readings were averaged every 24 h. A silver/silver chloride electrode was used to measure the individual electrode potentials. The coulombic efficiency (η_c) for a continuous flow, steady-state BES is the ratio of electrons for current flow to the maximum electron production (Logan et al. 2006) (Eq. 2).

$$\eta_c = \frac{M \cdot I}{F \cdot b \cdot q \cdot COD_\Delta} \qquad (2)$$

where M is the molecular weight of Cr$_2$O$_7$$^{2-}$ (2.16 × 10^5 mg mol^{-1}), I is the current (A), F is the Faraday constant (96,485.33 C mol^{-1}), b is the number of electrons exchanged per mole of Cr$_2$O$_7$$^{2-}$ reduced (6), q is the flow rate of the influent (L s^{-1}), and COD_Δ is the difference between the influent and effluent COD (mg L^{-1}).

Bacterial activity measurement

Because Cr(VI) is more toxic and soluble than Cr(III) (Jin et al. 2016, Vaiopoulou and Gikas 2012, Villaescusa et al. 1997), it is necessary to determine the change in bacterial activity while Cr(VI) is reduced. This study monitored the change in specific oxygen uptake rate (SOUR) of the sludge to assess the impact of Cr(VI) on bacterial activity. The SOUR was measured biweekly in duplicate following a previous protocol (Hu et al. 2002, Zhang et al. 2014).

Scanning electron microscopy (SEM)

The morphology and elemental composition of biofilms formed on the electrodes were analyzed by SEM coupled with energy-dispersive spectroscopy (EDS) (FEI Quanta 600 FEG Extended Vacuum SEM-EDS) after sample preparation at the University of Missouri (Columbia, MO). Sample preparation for microscopic analysis followed a previous protocol (Bozzola and Russell 1999, Zhang et al. 2019) with modifications. Briefly, sections of the electrodes from each bioreactor were cut and suspended overnight at 4 °C in a 0.1 M sodium cacodylate buffer (pH 7.5) containing 2% glutaraldehyde and 2% paraformaldehyde for primary fixation. The samples were rinsed three times by soaking for 5 min in a 0.1 M sodium cacodylate buffer and subsequently submerged in a 0.1 M sodium cacodylate buffer containing 2% osmium tetroxide for secondary fixation. The samples were then microwaved at 120 W (60 s off, 80 s on, 180 s off, and 40 s on), rinsed three times with the 0.1 M sodium cacodylate buffer and three times with deionized water, and dehydrated by passing through a series of solutions with increasing ethanol concentrations (20%, 50%, 70%, 90%, and 3 × 100%). The samples were finally prepared by CO_2 critical point dehydration before the SEM analysis.

Chemical analysis

Sludge volume index (SVI) and concentrations of NH_4^+-N, NO_3^--N, NO_2^--N, COD, orthophosphate (ascorbic acid method), Cr(VI) (1,5-diphenylcarbazide method), and biomass were measured twice a week according to the Standard Methods (APHA 2012). To differentiate the intracellular and extracellular total Cr, sludge samples were repeatedly washed using a trace metal cleaning reagent as described previously (Tovar-Sanchez et al. 2003). The wash liquid and the sludge were digested following a method described elsewhere (Zhang et al. 2014) and then analyzed for the concentrations of extracellular and intracellular total Cr, respectively, with a graphite furnace atomic absorption spectrophotometry (Buck Scientific, Inc., Norwalk, CT). For each sampling time and location (e.g., the influent and the effluent), two representative samples were taken for chemical analysis. The COD concentration of each sample was measured once, whereas the other wastewater constituents of each sample were determined twice (duplicate measurement).

Statistical analysis

Analysis of variance (ANOVA) was applied to determine whether the means of data sets (for COD, single measurement for each of the duplicate samples; for other constituents, duplicate measurements for each of the duplicate samples) are statistically significantly different. The significance level was 0.05.

Results and discussion

### Bioelectrochemical performance of the BESs

The three BESs attained a voltage of approximately 0.15 V 10 d after sludge seeding (Fig. 2). Following the dosing of Cr(VI) started on day 25 with increasing concentrations, the voltage of the MFCs increased to 0.33 ± 0.08 V with an average current of 0.34 mA and a power of 0.12 mW. Given the anode surface area of approximately 0.01 m^2, the continuous flow MFCs yielded current and power density of 33.6 mA m^{-2} and 11.2 ± 0.5 mW m^{-2}, respectively, when treating wastewater containing less than 10 mg L^{-1} of Cr(VI). This power density was lower than a previous report (i.e., 55 mW m^{-2}) (Tandukar et al. 2009). The low power generation could be attributed to several reasons. First, the synthetic wastewater had a higher resistance (approximately 1 mS cm^{-1}) than in other studies where high salt concentrations and buffer strengths were used (Rozendal et al. 2008). In addition, the electrode spacing ($\geq$ 5 cm) and the BES effective working volume (3.4 L) were considerably large, decreasing power generation (Cheng et al. 2006), whereas previous studies obtained high power densities with smal bioreactors (volumes less than 0.5 L) (Tandukar et al. 2009). Furthermore, over-potentials and ohmic losses due to resistance to flow of electrons and ions resulted in lower voltages. As a result, the coulombic efficiencies of the MFCs were only 13.3%.

Total Cr removal efficiency

The influent Cr(VI) concentrations peaked at 10 mg L^{-1} 75 d after BES setup (Fig. 3). The difference between influent and effluent Cr(VI) concentration was negligible at the beginning of Cr(VI) dosing (from day 25) due to the time required for sludge acclimation. Starting from day 41 (16 d after Cr(VI) dosing), the BESs began to reduce Cr(VI), resulting in lower effluent Cr(VI) concentrations.

During the start-up period, the MEC performed the best with effluent Cr(VI) concentration started to decrease from day 60 as compared with day 69 in the MFCs and day 74 in the control (Fig. 3). Biological Cr(VI) reduction in the BESs followed a first-order kinetics. The Cr(VI) reduction rate constant in the MEC was 0.103 d^{-1}. The MFCs with Cr(VI) fed to the anodic and the cathodic zones had comparable Cr(VI) reduction rate constants of 0.072 and 0.064 d^{-1}, respectively ($p = 0.29$, ANOVA). The control took more than 110 d to achieve complete Cr(VI) reduction with a much smaller reduction rate constant of 0.033 d^{-1}.

Fig. 2 Voltage (white and black circles) and current (white and black triangles) outputs from the MFCs. Open and close symbols depict the MFCs with Cr(VI) fed to the anodic and the cathodic zones, respectively.
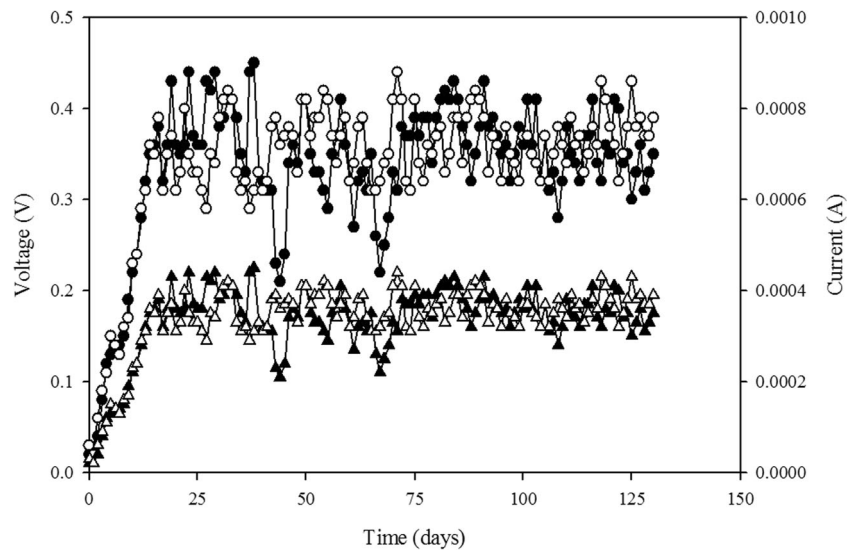

Total Cr removal mechanisms

The high Cr(VI) reduction rate in the BESs was due to the unique bioelectrochemical reactions on the electrodes where exoelectrogens delivered electrons to the anode and eventually to the cathode via an external circuit. This electron delivery facilitated microbial reduction of Cr(VI) (electron acceptor). The posed voltage in the MEC accelerated the growth of microorganisms which efficiently produced currents/electrons that were absent in abiotic controls (Huang et al. 2011a). Those additional electrons caused faster and more complete microbial Cr(VI) reduction in combination with abiotic electrochemical reduction of Cr(VI). The MFCs worked the same as the MEC except that the electrons were self-generated by the anode.

At the influent total Cr concentration of 10 mg L^{-1}, the MEC had the lowest effluent total Cr concentration with an overall removal efficiency of $66.2\% \pm 2.7\%$. Total Cr concentrations between the effluents of the two MFCs were not significantly different ($p = 0.82$, ANOVA), which had an overall removal efficiency of $56.7\% \pm 2.5\%$. For comparison, despite a complete reduction of Cr(VI), the control had the lowest total Cr removal efficiency ($26.1\% \pm 1.3\%$).

Total Cr was removed from the wastewater in all bioreactors, but its partitioning within bacteria and distribution in sludge remained to be explored. Intracellular and extracellular total Cr concentrations were, therefore, determined (Fig. 4). The intracellular and extracellular ratios of total Cr in the biomass for all BESs were not significantly different ($p = 0.20$ and 0.61 for the anodic and cathodic zones, respectively,

Fig. 3 Cr(VI) and total Cr concentrations in the influent and effluent of the BESs. Cr(VI): influent (black circle), effluent of the control (black down-pointing triangle), effluent of the MFC with Cr(VI) fed to the anodic zone (black square), effluent of the MFC with Cr(VI) fed in the cathodic zone (black diamond), and effluent of the MEC (black up-pointing triangle). Total Cr: influent (white circle), effluent of the control (white down-pointing triangle), effluent of the MFC with Cr(VI) fed to the anodic zone (white square), effluent of the MFC with Cr(VI) fed to the cathodic zone (white diamond), and effluent of the MEC (white down-pointing triangle).
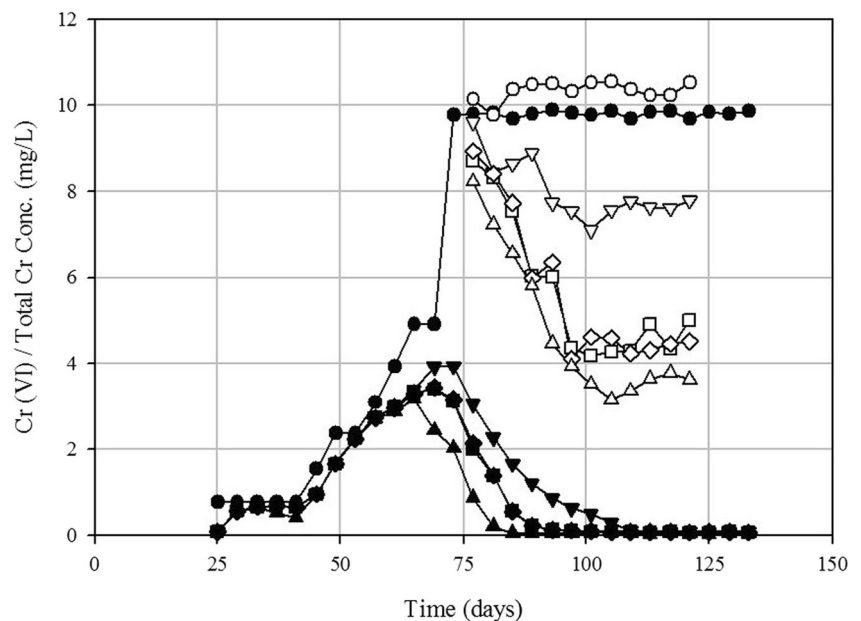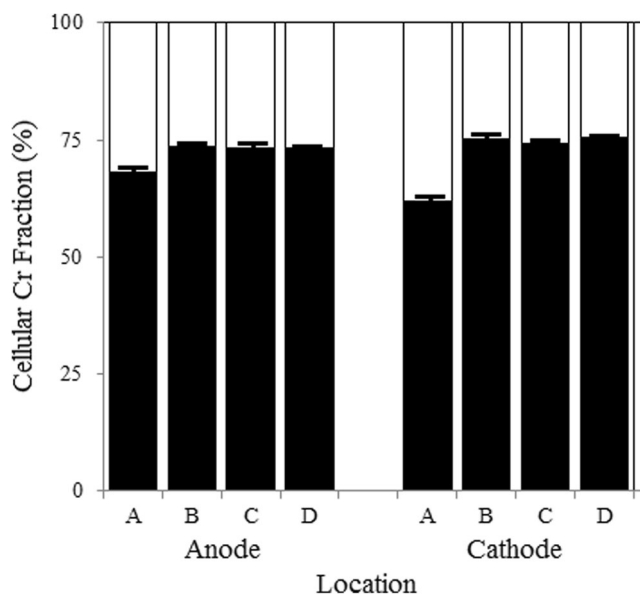
Fig. 4 Distribution of extracellular (black) and intracellular (white) total Cr in the sludge. (A) Control. (B) MFC with Cr(VI) fed to the anodic zone. (C) MFC with Cr(VI) fed to the cathodic zone. (D) MEC.

ANOVA), suggesting similarities in BES assisted Cr(VI) reduction and/or total Cr removal mechanisms. The intracellular Cr fraction averaged $26.7\% \pm 0.1\%$ and $25.1\% \pm 0.6\%$ for the anodic and cathodic zones for the BESs, respectively (Fig. 4). For comparison, the control showed a significantly higher ($p = 0.035$, ANOVA) intracellular total Cr accumulation with the fractions of $31.8\% \pm 1.4\%$ and $38.0\% \pm 0.9\%$ in the anodic and cathodic zones, respectively. These results suggest a joint Cr removal mechanism including Cr(VI) reduction (Song et al. 2016) via the carbon fiber/graphite cloth electrodes and Cr(III) precipitation in the BESs.

Cr precipitation in the biofilms on the electrodes was identified through SEM-EDS analysis (Fig. 5). Significant Cr deposited with phosphors on the electrodes as also reported in the literature (Huang et al. 2011a), suggesting the formation of Cr-phosphors coprecipitates and/or complexes. In contrast, on the electrodes of the control, the predominant elements were aluminum and sulfur without significant signal of Cr. These results along with the effluent Cr(VI) and total Cr concentrations indicate that, although Cr(VI) was reduced in the control with no bioelectrochemical functions, it was not captured as coprecipitates by the biofilms on the electrodes. In the BESs, however, the presence of exoelectrogens and their ability to bioelectrochemically reduce Cr(VI) resulted in a higher extracellular Cr accumulation (Fig. 5). The Cr(III) reduced from Cr(VI) could easily react with phosphors to form Cr-phosphors coprecipitates and/or complexes on the electrodes at neutral pH and be removed from the aqueous phase.

Wastewater treatment performance

At an average influent COD concentration of 512 mg L^{-1}, all BESs demonstrated a COD removal of 82% with no statistically significant difference ($p = 0.24$, ANOVA) (Fig. 6). The incremental dosing of Cr(VI) did not significantly hinder COD removal. Given the easily biodegradable nature of glucose, the relatively low COD removal efficiency was attributed to the non-aerated operation. This non-aeration practice was used to facilitate Cr(VI) reduction by avoiding competition for electrons between Cr(VI) and oxygen.

The bioreactors were initially fed with wastewater containing 20.9 ± 0.7 mg L^{-1} of NH_4^+-N. For the first 25 d of the operation, the effluent NH_4^+-N concentration was 8.4 ± 0.3 mg L^{-1}, suggesting nearly 60% of NH_4^+-N removal (Fig. 7). Following Cr(VI) dosing, the effluent NH_4^+-N concentration slightly increased to 10.5 ± 0.2 mg L^{-1} for days 25 to 60, indicating nitrification inhibition. Consistently, the autotrophic SOUR decreased from 15.8 ± 2.4 mg O$_2$ g^{-1} VSS h^{-1} at the beginning of the start-up period to 9.5 ± 2.6 mg O$_2$ g^{-1} VSS h^{-1} for days 25 to 60. The influent NH_4^+-N concentration was, therefore, reduced to 10 mg L^{-1} from day 61. Thereafter, the autotrophic SOUR resumed to 14.6 ± 3.3 mg O$_2$ g^{-1} VSS h^{-1} in the following 30 d, and the effluent NH_4^+-N concentration dropped to nearly zero (Fig. 7), suggesting biomass activity recovery and acclimatization. The effluent NH_4^+-N concentrations among the BESs were not significantly different.

The inoculum sludge had significant residual NO_3^--N (6.6 ± 0.6 mg L^{-1}) and caused a temporary accumulation of NO_2^--N (0.15 ± 0.03 mg L^{-1}) at the beginning of the start-up period (Fig. 7). However, nitrite and nitrate concentrations decreased steadily through continuous flow operation, suggesting stable and efficient nitrification/denitrification of the BESs despite no aeration. The average dissolved oxygen concentrations in the anodic, cathodic, and settling zones were 0.08 ± 0.03, 0.65 ± 0.10, and 0.38 ± 0.07 mg L^{-1}, respectively. The primary source of oxygen in the BESs was its dissolution in the settling zone and diffusion via stirring in the cathodic zone. The average effluent NO_3^--N concentration in the MEC was statistically significantly lower than those in the MFCs ($p < 0.001$, ANOVA). Furthermore, the BESs had much lower effluent NO_3^--N concentrations than the control ($p < 0.001$, ANOVA).

The enhanced NO_3^--N removal in the BESs was attributed to the exoelectrogenic bacteria enriched on the electrodes that reduced nitrate to nitrogen gas (Clauwaert et al. 2007, Virdis et al. 2010). The MEC performed better than the MFCs in reducing NO_3^--N and NO_2^--N due to the external electron supply. Despite the high nitrate removal efficiency, NO_3^--N in the BESs could still significantly reduce the coulombic efficiency and Cr(VI) reduction rate due to the competition

Bioreactor   **SEM Images**   **EDS Spectra**

Control
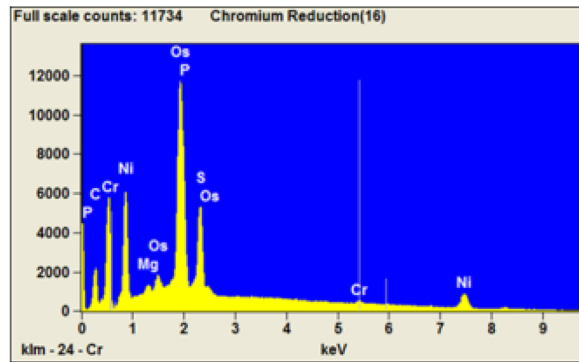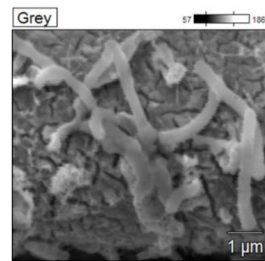
(Open Circuit)
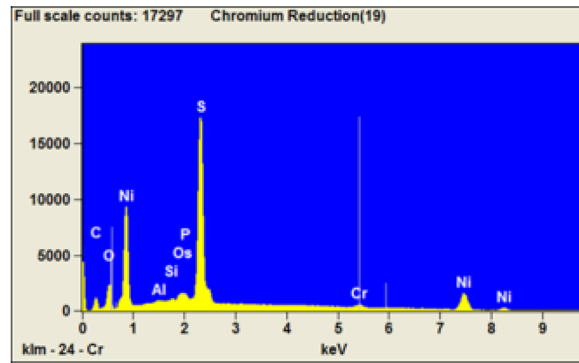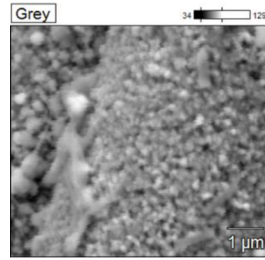
BESs

Fig. 5 SEM-EDS analysis of the biofilms on the electrodes. BESs stand for both MFCs and MEC. The SEM images and the EDS spectra show the biofilm morphology and the biofilm elemental composition, respectively. Size bars (1 μm) are shown in the SEM photomicrographs. The adjacent high peaks for phosphors and Cr of the biofilms in the BESs (EDS spectra) indicate the formation of Cr(III)-phosphors coprecipitates and/or complexes.

between Cr(VI) and nitrate for electrons (Sukkasem et al. 2008). Therefore, to avoid the accumulation of NO_3^--N, the influent NH_4^+-N concentration was reduced to 9.4 ± 0.3 mg L^{-1} from day 61. The effluent NO_3^--N concentration dramatically reduced to 0.07 ± 0.03 mg L^{-1} thereinafter (Fig. 7), indicating complete denitrification.

Fig. 6 COD concentrations in the influent (black square) and effluent of the BESs. Effluent: control (black circle); MFC with Cr(VI) fed to the anodic zone (white circle); MFC with Cr(VI) fed to the cathodic zone (black down-pointing triangle); and MEC (white up-pointing triangle). Error bars represent the half ranges of duplicate samples (COD concentration was measured once for each of the duplicate samples).
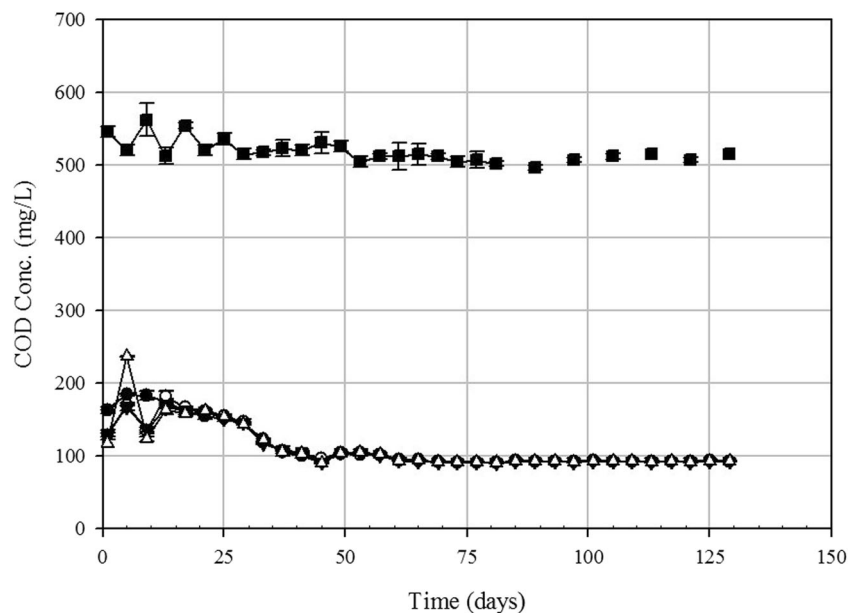
Fig. 7 Nitrogen species (ammonium, nitrate, and nitrite) concentrations in the influent (black square) and effluent of the BESs. Effluent: control (black circle); MFC with Cr(VI) fed to the anodic zone (white circle); MFC with Cr(VI) fed to the cathodic zone (black down-pointing triangle); and MEC (white up-pointing triangle). Error bars represent the standard deviations of duplicate samples (nitrogen species concentration was measured twice for each of the duplicate samples).
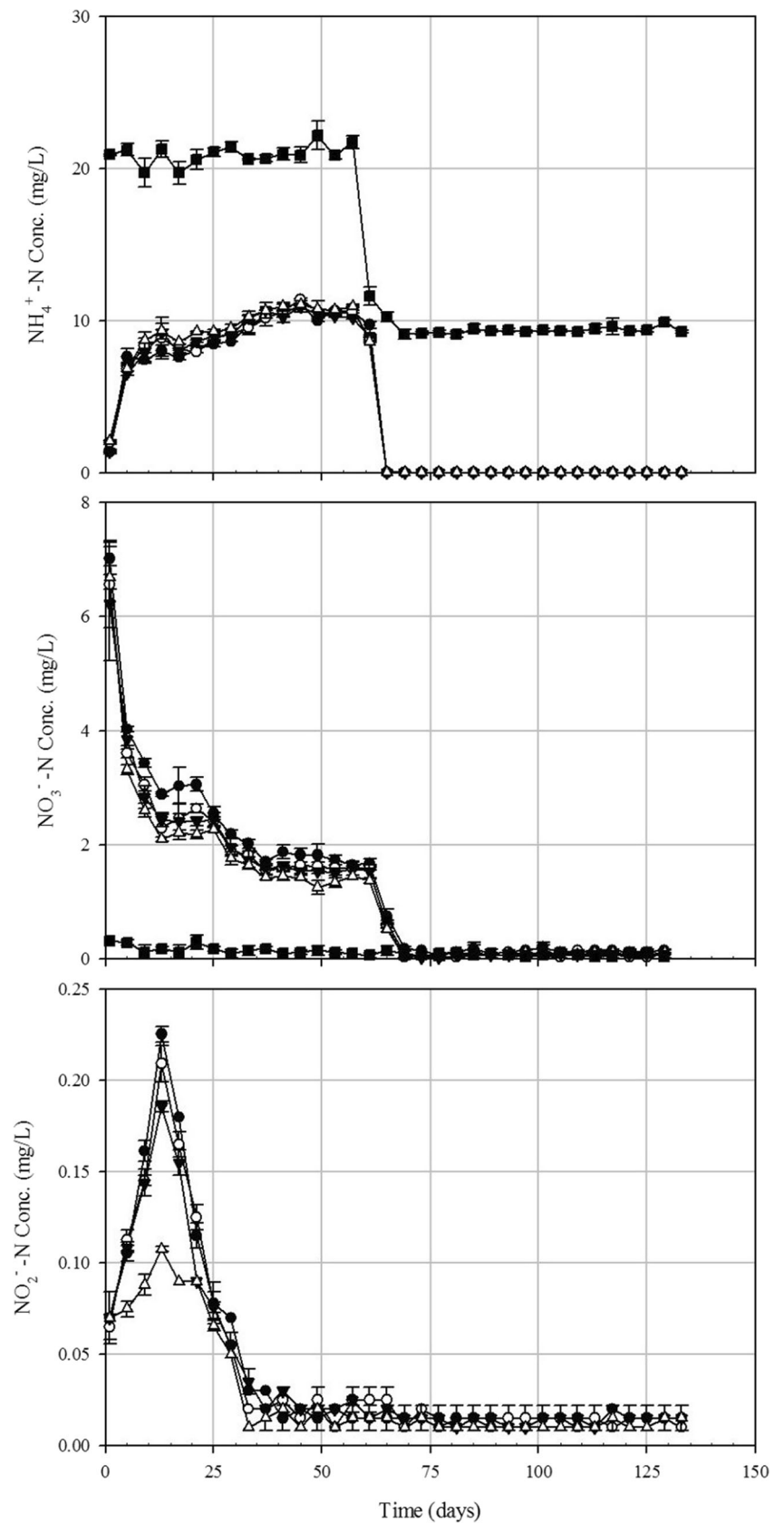
Implications and prospects of the BESs for Cr removal

BESs have showed their feasibility to reduce Cr(VI) and remove total Cr from wastewater mostly in small, batch systems (Gupta et al. 2017, Habibul et al. 2016, Huang et al. 2015, Song et al. 2016, Wang et al. 2017). This study demonstrated the capability of large, continuous flow BESs with low-cost electrodes for fast Cr(VI) reduction and improved total Cr removal. Without any proton exchange membrane, our BESs still effectively reduced Cr(VI) and removed total Cr from wastewater, which is expected to detoxify Cr(VI). Compared to the control and the MFCs, the MEC not only demonstrated faster Cr(VI) reduction, but also exhibited a much higher total Cr removal efficiency due to the external power supply. Meanwhile, the reduced Cr coprecipitated with phosphorus in the biomass/sludge can be easily recovered or disposed of. Those added benefits could offset the financial burden of using electrodes and maintaining the BESs. Further research is needed to recover Cr from the sludge before final disposal.

The MFCs demonstrated a maximum power density of 11.2 ± 0.5 mW m^{-2} and a low coulombic efficiency of 13.3%. This low coulombic efficiency can be attributed to multiple factors such as the specific reactor configuration (e.g., over-potentials caused by large reactor), the low-cost electrodes, and the presence of competing electron acceptors (e.g., nitrate). Further material and reactor configuration improvements are needed before BESs can be implemented for Cr(VI) reduction and total Cr removal in full-scale wastewater treatment facilities.

Conclusions

This study demonstrated the feasibility of simple, large, cost-effective, continuous flow BESs with neither cathode catalyst nor proton exchange membrane in reducing Cr(VI) and removing total Cr from wastewater. The BESs promoted Cr(VI) (electron acceptor) reduction on the cathode by providing electrons and facilitated total Cr removal through coprecipitation of Cr(III) and phosphors with the biomass. The bioreactor configurations significantly affected the performance of the BESs. Due to the external power supply, the MEC was more efficient than the MFCs in Cr(VI) reduction and total Cr removal. The first-order Cr(VI) reduction rate constant for the MEC was 0.103 d^{-1}, higher than those of the MFCs (≤ 0.072 d^{-1}). The MEC also had a higher total Cr removal (66.2%) than the MFCs (56.7%). For comparison, the control had a much lower first-order Cr(VI) reduction rate constant (0.033 d^{-1}) and total Cr removal (26.1%). In summary, the MEC had the fastest Cr(VI) reduction and highest total Cr removal. In addition, biomass in the BESs had lower intracellular Cr contents than the control.

Compliance with ethical standards

References

Al-Shannag M, Al-Qodah Z, Bani-Melhem K, Qtaishat MR, Alkasrawi M (2015) Heavy metal ions removal from metal plating wastewater using electrocoagulation: kinetic study and process performance. *Chem Eng J* 260:749–756

APHA (2012) *Standard Methods for the Examination of Water and Wastewater*, American Public Health Association (APHA), American Water Works Association (AWWA), and Water Environment Federation (WEF), 22nd edn, Washington, DC, USA

Arias YM, Tebo BM (2003) Cr(VI) reduction by sulfidogenic and nonsulfidogenic microbial consortia. *Appl Environ Microbiol* 69(3):1847–1853

Bozzola JJ, Russell LD (1999) *Electron Microscopy: Principles and Techniques for Biologists*, 2nd edn. Jones and Bartlett Publishers, Inc, Boston, USA

Buerge IJ, Hug SJ (1997) Kinetics and pH dependence of chromium(VI) reduction by iron(II). *Environ Sci Technol* 31(5):1426–1432

Cheballah K, Sahmoune A, Messaoudi K, Drouiche N, Lounici H (2015) Simultaneous removal of hexavalent chromium and COD from industrial wastewater by bipolar electrocoagulation. *Chem Eng Process* 96:94–99

Chen JM, Hao OJ (1998) Microbial chromium (VI) reduction. *Crit Rev Environ Sci Technol* 28(3):219–251

Cheng S, Liu H, Logan BE (2006) Increased power generation in a continuous flow MFC with advective flow through the porous anode and reduced electrode spacing. *Environ Sci Technol* 40(7):2426–2432

Clauwaert P, Rabaey K, Aelterman P, De Schamphelaire L, Pham TH, Boeckx P, Boon N, Verstraete W (2007) Biological denitrification in microbial fuel cells. *Environ Sci Technol* 41(9):3354–3360

Eary LE, Rai D (1987) Kinetics of chromium(III) oxidation to chromium(VI) by reaction with manganese dioxide. *Environ Sci Technol* 21(12):1187–1193

Gajaraj S, Hu Z (2014) Integration of microbial fuel cell techniques into activated sludge wastewater treatment processes to improve nitrogen removal and reduce sludge production. *Chemosphere* 117:151–157

Gregory KB, Lovley DR (2005) Remediation and recovery of uranium from contaminated subsurface environments with electrodes. *Environ Sci Technol* 39(22):8943–8947

Gupta S, Yadav A, Verma N (2017) Simultaneous Cr(VI) reduction and bioelectricity generation using microbial fuel cell based on alumina-nickel nanoparticles-dispersed carbon nanofiber electrode. *Chem Eng J* 307:729–738

Habibul N, Hu Y, Wang YK, Chen W, Yu HQ, Sheng GP (2016) Bioelectrochemical chromium(VI) removal in plant-microbial fuel cells. *Environ Sci Technol* 50(7):3882–3889

Han R, Li F, Liu T, Li X, Wu Y, Wang Y, Chen D (2016) Effects of incubation conditions on Cr(VI) reduction by *c*-type cytochromes in intact *Shewanella oneidensis* MR-1 cells. *Front Microbiol* 7:746

Hosseini MS, Belador F (2009) Cr(III)/Cr(VI) speciation determination of chromium in water samples by luminescence quenching of quercetin. *J Hazard Mater* 165(1-3):1062–1067

Hu Z, Chandran K, Grasso D, Smets BF (2002) Effect of nickel and cadmium speciation on nitrification inhibition. *Environ Sci Technol* 36(14):3074–3078

Huang L, Chen J, Quan X, Yang F (2010) Enhancement of hexavalent chromium reduction and electricity production from a biocathode microbial fuel cell. *Bioprocess Biosyst Eng* 33(8):937–945

Huang L, Chai X, Chen G, Logan BE (2011a) Effect of set potential on hexavalent chromium reduction and electricity generation from biocathode microbial fuel cells. *Environ Sci Technol* 45(11):5025–5031

Huang L, Cheng S, Chen G (2011b) Bioelectrochemical systems for efficient recalcitrant wastes treatment. *J Chem Technol Biotechnol* 86(4):481–491

Huang L, Wang Q, Jiang L, Zhou P, Quan X, Logan BE (2015) Adaptively evolving bacterial communities for complete and selective reduction of Cr(VI), Cu(II), and Cd(II) in biocathode bioelectrochemical systems. *Environ Sci Technol* 49(16):9914–9924

Ishibashi Y, Cervantes C, Silver S (1990) Chromium reduction in *Pseudomonas putid*. *Appl Environ Microbiol* 56(7):2268–2270

Jin W, Du H, Zheng S, Zhang Y (2016) Electrochemical processes for the environmental remediation of toxic Cr(VI): a review. *Electrochim Acta* 191:1044–1055

Li Z, Zhang X, Lei L (2008) Electricity production during the treatment of real electroplating wastewater containing Cr^{6+} using microbial fuel cell. *Process Biochem* 43(12):1352–1358

Li M, Zhou S, Xu Y, Liu Z, Ma F, Zhi L, Zhou X (2018) Simultaneous Cr(VI) reduction and bioelectricity generation in a dual chamber microbial fuel cell. *Chem Eng J* 334:1621–1629

Liang Z, Hu Z (2012) Start-up performance evaluation of submerged membrane bioreactors using conventional activated sludge process and modified Luzack-Ettinger process. *J Environ Eng* 138(9):932–939

Liu C, Gorby YA, Zachara JM, Fredrickson JK, Brown CF (2002) Reduction kinetics of Fe(III), Co(III), U(VI), Cr(VI), and Tc(VII) in cultures of dissimilatory metal-reducing bacteria. *Biotechnol Bioeng* 80(6):637–649

Liu L, Yuan Y, Li F, Feng C (2011) *In-situ* Cr(VI) reduction with electrogenerated hydrogen peroxide driven by iron-reducing bacteria. *Bioresour Technol* 102(3):2468–2473

Liu W, Ni J, Yin X (2014) Synergy of photocatalysis and adsorption for simultaneous removal of Cr (VI) and Cr (III) with TiO_2 and titanate nanotubes. *Water Res* 53:12–25

Logan BE, Hamelers B, Rozendal R, Schröder U, Keller J, Freguia S, Aelterman P, Verstraete W, Rabaey K (2006) Microbial fuel cells: methodology and technology. *Environ Sci Technol* 40(17):5181–5192

Lovley DR, Phillips EJP, Gorby YA, Landa ER (1991) Microbial reduction of uranium. *Nature* 350(6317):413–416

Lu J, Wang Z, Liu Y, Tang Q (2016) Removal of Cr ions from aqueous solution using batch electrocoagulation: Cr removal mechanism and utilization rate of in situ generated metal ions. *Process Saf Environ Prot* 104:436–443

Mandiwana K, Panichev N, Kataeva M, Siebert S (2007) The solubility of Cr(III) and Cr(VI) compounds in soil and their availability to plants. *J Hazard Mater* 147(1-2):540–545

Mohan D, Pittman CU Jr (2006) Activated carbons and low cost adsorbents for remediation of tri- and hexavalent chromium from water. *J Hazard Mater* 137(2):762–811

Nancharaiah Y, Mohan SV, Lens P (2015) Metals removal and recovery in bioelectrochemical systems: a review. *Bioresour Technol* 195:102–114

Pandit S, Sengupta A, Kale S, Das D (2011) Performance of electron acceptors in catholyte of a two-chambered microbial fuel cell using anion exchange membrane. *Bioresour Technol* 102(3):2736–2744

Qin G, McGuire MJ, Blute NK, Seidel C, Fong L (2005) Hexavalent chromium removal by reduction with ferrous sulfate, coagulation, and filtration: a pilot-scale study. *Environ Sci Technol* 39(16):6321–6327

Rai D, Eary L, Zachara JM (1989) Environmental chemistry of chromium. *Sci Total Environ* 86(1-2):15–23

Rozendal RA, Hamelers HVM, Rabaey K, Keller J, Buisman CJN (2008) Towards practical implementation of bioelectrochemical wastewater treatment. *Trends Biotechnol* 26(8):450–459

Rutigliano L, Fino D, Saracco G, Specchia V, Spinelli P (2008) Electrokinetic remediation of soils contaminated with heavy metals. *J Appl Electrochem* 38(7):1035–1041

Schmieman EA, Yonge DR, Rege MA, Petersen JN, Turick CE, Johnstone DL, Apel WA (1998) Comparative kinetics of bacterial reduction of chromium. *J Environ Eng* 124(5):449–455

Song T, Jin Y, Bao J, Kang D, Xie J (2016) Graphene/biofilm composites for enhancement of hexavalent chromium reduction and electricity production in a biocathode microbial fuel cell. *J Hazard Mater* 317:73–80

Sukkasem C, Xu S, Park S, Boonsawang P, Liu H (2008) Effect of nitrate on the performance of single chamber air cathode microbial fuel cells. *Water Res* 42(19):4743–4750

Tandukar M, Huber SJ, Onodera T, Pavlostathis SG (2009) Biological chromium(VI) reduction in the cathode of a microbial fuel cell. *Environ Sci Technol* 43(21):8159–8165

Tebo BM, Obraztsova AY (1998) Sulfate-reducing bacterium grows with Cr(VI), U(VI), Mn(IV), and Fe(III) as electron acceptors. *FEMS Microbiol Lett* 162(1):193–198

Tovar-Sanchez A, Sañudo-Wilhelmy SA, Garcia-Vargas M, Weaver RS, Popels LC, Hutchins DA (2003) A trace metal clean reagent to remove surface-bound iron from marine phytoplankton. *Mar Chem* 82(1-2):91–99

Vainshtein M, Kuschk P, Mattusch J, Vatsourina A, Wiessner A (2003) Model experiments on the microbial removal of chromium from contaminated groundwater. *Water Res* 37(6):1401–1405

Vaiopoulou E, Gikas P (2012) Effects of chromium on activated sludge and on the performance of wastewater treatment plants: a review. *Water Res* 46(3):549–570

Villaescusa I, Marti S, Matas C, Martine M, Ribó JM (1997) Chromium(VI) toxicity to luminescent bacteria. *Environ Toxicol Chem* 16(5):871–874

Virdis B, Rabaey K, Rozendal RA, Yuan Z, Keller J (2010) Simultaneous nitrification, denitrification and carbon removal in microbial fuel cells. *Water Res* 44(9):2970–2980

Wang H, Ren ZJ (2014) Bioelectrochemical metal recovery from wastewater: a review. *Water Res* 66:219–232

Wang G, Huang L, Zhang Y (2008) Cathodic reduction of hexavalent chromium [Cr(VI)] coupled with electricity generation in microbial fuel cells. *Biotechnol Lett* 30(11):1959–1966

Wang H, Luo H, Fallgren PH, Jin S, Ren ZJ (2015) Bioelectrochemical system platform for sustainable environmental remediation and energy generation. *Biotechnol Adv* 33(3):317–334

Wang Q, Huang L, Pan Y, Quan X, Li Puma G (2017) Impact of Fe(III) as an effective electron-shuttle mediator for enhanced Cr(VI) reduction in microbial fuel cells: reduction of diffusional resistances and cathode overpotentials. *J Hazard Mater* 321:896–906

Wu S, Ge Y, Wang Y, Chen X, Li F, Xuan H, Li X (2018) Adsorption of Cr(VI) on nano Uio-66-NH_2 MOFs in water. *Environ Technol* 39(15):1937–1948

Xu C, Yang W, Liu W, Sun H, Jiao C, Lin A (2018) Performance and mechanism of Cr(VI) removal by zero-valent iron loaded onto expanded graphite. *J Environ Sci* 67:14–22

Zhang C, Liang Z, Hu Z (2014) Bacterial response to a continuous long-term exposure of silver nanoparticles at sub-ppm silver concentrations in a membrane bioreactor activated sludge system. *Water Re*s 50:350–358

Zhang C, Brown PJ, Miles RJ, White TA, Grant DG, Stalla D, Hu Z (2019) Inhibition of regrowth of planktonic and biofilm bacteria after peracetic acid disinfection. *Water Res* 149:640–649

Zhou L, Li R, Zhang G, Wang D, Cai D, Wu Z (2018) Zero-valent iron nanoparticles supported by functionalized waste rock wool for efficient removal of hexavalent chromium. *Chem Eng J* 339:85–96